

**Field enhancement and rectification of surface plasmons detected by scanning tunneling microscopy**Miklós Lenner,<sup>1,2,\*</sup> Péter Rácz,<sup>1</sup> Péter Dombi,<sup>1</sup> Győző Farkas,<sup>1</sup> and Norbert Kroó<sup>1</sup><sup>1</sup>Research Institute for Solid-State Physics and Optics, H-1121 Budapest, Konkoly-Thege M. út 29-33, Hungary<sup>2</sup>ABB Switzerland Ltd., Corporate Research Center, CH-5405 Baden-Dättwil, Switzerland

(Received 23 October 2010; revised manuscript received 22 December 2010; published 25 May 2011)

We investigated surface plasmon (SP) waves in the junction of a scanning tunneling microscope (STM). The SP waves were generated on a 45-nm thin Au film and their near-field was locally probed by the tip of the STM. The temporal structure of the observed tunneling current signal revealed information on the physical mechanisms which regulate the interaction of the electric fields in play. We estimated the magnitude of the local electric field enhancement on surface nanostructures by taking advantage of the nonlinearity of the tunneling junction. The mapping of the plasmon field to the surface topography delivers experimental evidence for the localization of SP waves in narrow gaps of a few nanometers width and/or at grain boundaries. The results gained can directly be utilized (e.g., in the development of nanoscale geometries for high-energy electron sources where electrons are accelerated in the electric field of surface plasmons).

DOI: [10.1103/PhysRevB.83.205428](https://doi.org/10.1103/PhysRevB.83.205428)

PACS number(s): 73.20.Mf, 42.50.-p, 68.37.-d, 78.67.-n

**I. INTRODUCTION**

The fascinating properties of the tunneling junction of a scanning tunneling microscope (STM) have sparked a surge of research interest in the past. Its nonlinear response facilitates not only atomic resolution on surfaces<sup>1</sup> but also allows, for example, for atomic manipulation,<sup>2</sup> laser frequency mixing,<sup>3</sup> microwave generation,<sup>4</sup> or rectification on the atomic scale<sup>5</sup> when interacting with external electromagnetic radiation.

When surface plasmons (SPs) are excited in the tunneling junction, the electric field of these resonantly excited collective oscillation modes of the conduction electrons additionally contributes to the tunneling current that results from the electronic DC bias.<sup>6</sup> In this case, the SPs are usually excited optically on the metal surface (e.g., by laser irradiation) in appropriate geometry.<sup>7</sup> The superimposed portion of the tunneling current is only present in existence of the SP field and is (unlike current components generated by thermal effects) independent of the bias polarity. Due to the nonlinear characteristics of the tunneling junction it manifests as a rectified DC component in the tunneling current and can be used as a measure for the SP amplitude. Note that there are alternative methods for the detection of SP fields (e.g.,<sup>8,9</sup>).

On the other hand, the research of ultrafast monoenergetic electron sources calls for a characterization tool that is capable of delivering information on the *local* behavior of SP waves. These novel sources take advantage of the ponderomotive acceleration of photoelectrons that occurs in the evanescent field of surface plasmon waves.<sup>10</sup> It has been shown that, in addition to the optical waveform control, nanoscale surface geometry has a key influence on the electron emission properties.<sup>11</sup> A recent study of the electromagnetic response in a plasmonic nanogap demonstrated that the field enhancement can exceed three orders of magnitude in a purpose-built surface geometry.<sup>12</sup> The field enhancement was quantified via optical rectification.

Here, we present a study of the interaction of surface plasmon waves within the tunneling junction of a scanning tunneling microscope by locally probing their near-field. The

experimental arrangement allows for the study of *arbitrary* surface geometries that are plasmonically active.

First, we demonstrate different signal types in the time domain and connect them with the physical mechanisms by which they have been generated. In the Bias analysis section, we investigate the interaction between the field of the STM tip and the SP waves and show their influence on the tunneling current. In Sec. III C we analyze the pulse energy dependence in the framework of an analytical model and compare the results with experimental data. In addition, we estimate the magnitude of the local field enhancement. Finally, in Sec. III D we map the localized electric field of the plasmons and connect them with the surface topography.

**II. EXPERIMENTAL**

The measuring principle of the system used has been described elsewhere.<sup>13</sup> Briefly, the surface plasmons were generated on a vacuum-evaporated gold film of 45-nm thickness in Kretschmann geometry<sup>7</sup> in order to minimize thermal effects. The laser pulses were produced by an electronically gated semiconductor diode (central wavelength  $\lambda_0 = 670$  nm, pulse duration  $\tau_p = 50$   $\mu$ s, repetition rate  $f_{\text{rep}} = 1$  kHz) and focused tightly by an  $f = 30$ -mm lens onto the target. The STM was operated in constant current mode. The tunneling current was processed by a low-noise current-to-voltage converter and subsequently amplified by a factor of  $10^9$ . The electronic response of the amplifier was recorded by an A/D converter at a sampling rate of  $f_s = 500$  kHz for *in situ* analysis. In addition, the signal passed an integrator stage and was fed into the height-control loop of the surface topography signal. Digital signal processing allowed the enhancement of the signal-to-noise ratio as well as long-term stability. Both W and Au tips were used in the experiments.

As for the bias voltage dependence measurements, the surface scanning was stopped and the sample-to-tip distance was kept constant by turning the feedback loop off during the measurement. However, in order to avoid  $z$  drift, the distance was reset between each of the measured bias voltages.

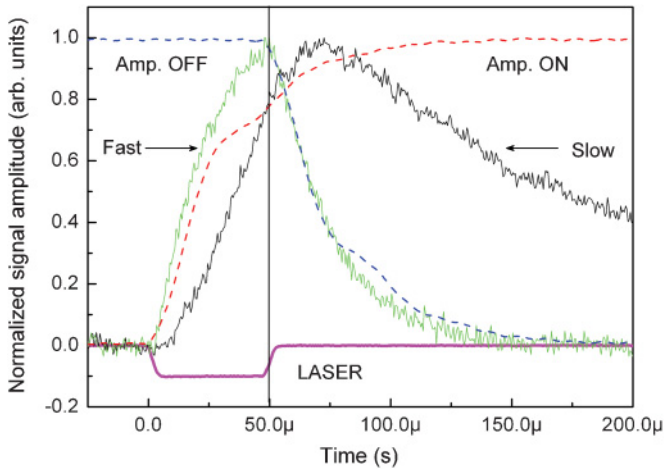


FIG. 1. (Color online) Typical signal forms during surface scans. The amplitudes of the “Slow” and “Fast” types of signals (solid black and green curves, respectively) are normalized (and the “Fast” type of signal additionally inverted) for comparison. The “Amp. ON” and “Amp. OFF” signals (dashed red and blue curves, respectively) represent the normalized step response of the current amplifier (see parameters in text). The “Laser” signal (thick magenta line) is displayed inverted for clarity.

### III. RESULTS AND DISCUSSION

#### A. Time domain analysis

Two typical signal forms (labeled as “Slow” and “Fast”, respectively) of the normalized tunneling current observed at certain surface locations are shown in Fig. 1 along with the laser monitor signal. The level of the observed tunneling signals was different; peak currents were measured up to a few hundred picoamperes. In addition, the measured electronic response of the current-to-voltage converter/amplifier is displayed (denoted as “Amp. ON” and “Amp. OFF”) when a step function ( $I_{\text{peak-to-peak}} = 400 \text{ pA}$ ,  $\tau_{\text{rise}} = \tau_{\text{fall}} = 300 \text{ ns}$ ) was

applied on the input terminal. The amplitude of the test signal corresponds to typical values obtained during operation.

The “Slow” type of signal is typical for the case when the modulation of the tunneling current is dominated by thermal effects.<sup>14</sup> The maximum amplitude of the signal is reached in a few tens of microseconds *after* the laser pulse is switched off due to the heat diffusion/thermal relaxation dynamics of the tip. The time constant of the signal change ( $\sim 100 \mu\text{s}$ ) suggests that the main contribution of the thermal expansion originates from the STM tip<sup>15</sup> and the expansion of the sample may not be dominant.<sup>16</sup> Both the leading and the trailing edge of the tunneling signal are significantly slower than the electronic response of the amplifier.

In contrast, the second type of signal (denoted as “Fast”) was detected only at specific surface locations. It is characterized by very fast rise and fall times which are on the time scale of the temporal resolution of the amplifier used. The maximum of the signal is reached at the “end” of the SP excitation and it starts to decrease instantly as soon as the light source is switched off. Obviously, due to the relatively low bandwidth limit of the amplifier, we cannot gain insight into the exact temporal evolution of the process which generates this modulation in the tunneling current. However, this signal is clearly faster than that of the “Slow” type and its rise time is shorter or equal to that of the amplifier. It suggests that the current modulation is caused predominantly by fast surface electronic processes (e.g., the electric field of localized surface plasmons) rather than by relatively slow, thermal processes.

#### B. Bias voltage dependence

In order to gain more insight into the origin of different signal types we performed a bias voltage scan at a constant surface location. The tip-sample distance was kept constant by resetting it for each bias voltage. In addition, we kept the measurement times as short as possible (in the order of a few seconds) to avoid lateral drifts. The results of the measurements are summarized in Fig. 2.

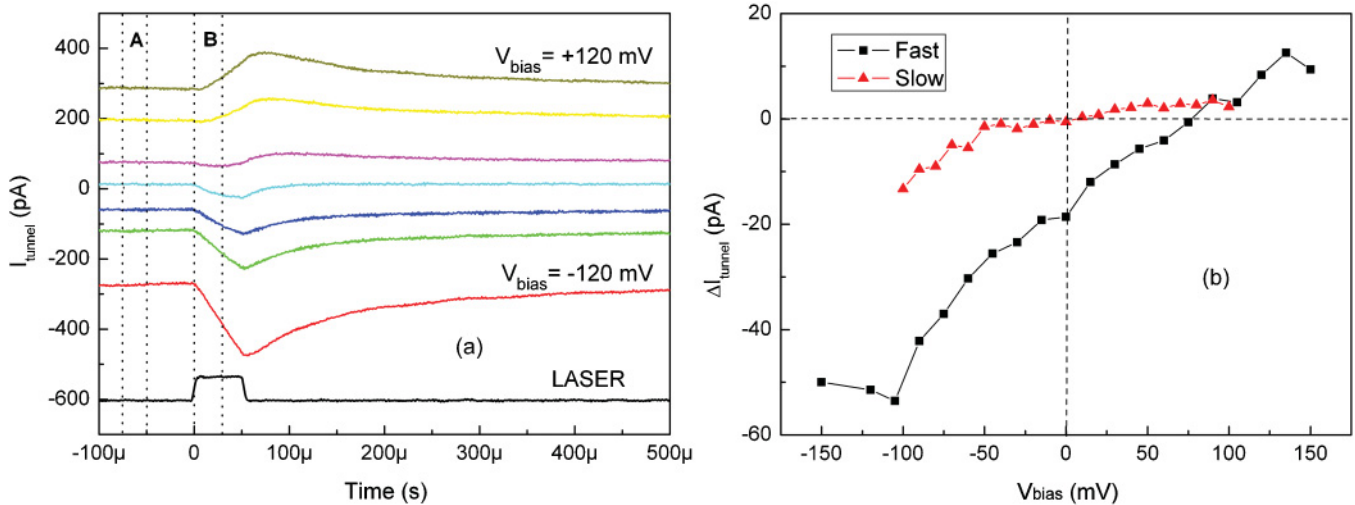


FIG. 2. (Color online) (a) Bias voltage scan at a constant surface location for “Fast” type of signal. Displayed  $V_{\text{bias}}$  values are  $-120, -90, -30, 0, 30, 90,$  and  $120 \text{ mV}$ . The markers A and B represent the time gates (integration intervals) for the background and plasmon signal contributions, respectively. The black squares in Fig. 2(b) display the SP-induced *change* of the tunneling current from Fig. 2(a) by applying appropriate transformation (see text). The red triangles show the result of the same transformation applied for “Slow” types of signals.

Figure 2(a) shows the time evolution of the tunneling current for “Fast”-type signals as a function of time and the bias voltage ranging from  $-120$  mV to  $+120$  mV. We also show the position of the time gates (being gate A the Background and gate B the plasmon contribution, respectively). Again, we assume here that during SP excitation, the modulation of the tunneling signal is dominated by the surface electric field. We integrated the signals in the set time windows and subtracted the integral background contribution of gate A from that of gate B, as a function of  $V_{\text{bias}}$ . This transformation allowed us to determine the differential characteristics of the tunneling junction which is depicted in Fig. 2(b). The curves here represent the *change* of the tunneling current due to the SP field as a function of the bias voltage. As for the “Slow” type of signal, the differential characteristic was nearly zero (within 2% accuracy) at  $V_{\text{bias}} = 0$  V in *each* measurement. This means that the SP-induced contribution was equal to the background (time integral of gate A) in the case of the absence of an external static electric field—in line with theoretical predictions.<sup>17</sup> For  $V_{\text{bias}} \neq 0$  the change of the integrated tunneling current is proportional to the applied field. As the pulse-to-pulse thermal expansion is essentially constant at a certain laser pulse energy level, this observation suggests that the signal modulation originates dominantly from thermal effects in the tunneling junction.

On the other hand, the “Fast” signal is clearly negative at zero bias and has a zero crossing at significantly higher bias values (typically a few tens of millivolts, always positive). In other words, in the presence of the laser-induced plasmon field there must be an electric field generated which equilibrates with the electric field of the biased tip at  $V_{\text{bias}} > 0$ . What could be the origin of this field?

One possible explanation could be the existence of the contact potential which is generally present at the junction of two metals of different work functions (that is 4.5 eV for W and 4.3 eV for Au).<sup>18</sup> Therefore, the experiments were also performed with Au tip on Au surface. As a result, we were able to find both “Fast” and “Slow” types of signals. Even though “Fast”-type signals appear less frequently (due to lower tip sharpness that was reflected in lower topography resolution), their existence suggests that the origin of these signals cannot be due to local variations of the contact potential. In addition, none of the typical signal types have been observed in the absence of the SP field. Due to the long pulse duration ( $\tau_p = 50$   $\mu$ s) the laser field was relatively low (in the order of a few kV/cm) and was therefore unlikely to directly influence the tunneling properties.

Thus, we believe that the field in question originates from the combination of the rectification in the tunneling junction<sup>19</sup> and the local surface electric field enhancement.<sup>20</sup> It is well known that the electric field can be orders of magnitude higher on nanometer-scale structures such as nanocavities,<sup>21</sup> nanogaps, or spheres.<sup>22</sup> According to these calculations the field enhancement can be sufficient enough to amplify the laser-induced plasmon field by three to four orders of magnitude in the proximity of these nanostructures. Due to the nonlinear characteristics of the tunneling junction, the amplified electric field of the plasmons can be rectified.<sup>23</sup> This rectified portion creates a quasistatic (DC) voltage across the junction in the presence of the SP excitation. The amount

and the sign of the rectified voltage can be characterized by the  $I$ - $V$  characteristics of the junction.<sup>4</sup> As thermal expansion may take place all over the laser-illuminated sample area, it cannot be excluded that signatures of the “Slow” type of signal are present in the “Fast” one. However, the level of the “Slow” signal can be lower by up to one order of magnitude [see Fig. 2(b)]. The separation of particular signal contributions represents thus a challenging task.

### C. Pulse energy dependence

We studied the evolution of the tunneling current as a function of the laser pulse energy for the “Fast” type of signals in the *absence* of external electric fields (i.e.,  $V_{\text{bias}} = 0$  V). At the same time, we calculated the tunneling current resulting from the rectification of the surface plasmon field. The results are displayed in Fig. 3. The rectification of optical<sup>4</sup> and plasmon<sup>6</sup> fields was studied in previous works. Here, we vary the amplitude of the SP-generating optical field and show the nonlinear dependence of the change of the tunneling current which gives a direct indication for the amplitude of the rectified SP field. In the calculation we assume that the origin of the rectification effect is based on the nonlinearity of the static  $I$ - $V$  characteristics. This means that the time response of the tunneling junction must be fast enough for the rectification of optical frequencies.<sup>4</sup>

Given the measured static characteristics  $I_{\text{stat}}(V_{\text{bias}})$  (shown in the inset of Fig. 3) obtained from the gate signal “A” in Fig. 2(a) one can determine the resulting rectified DC current as the time average of the optically induced AC current by

$$I_{\text{rect}}(\hat{V}_{\text{opt}}) = \frac{\omega}{2\pi} \int_0^{2\pi/\omega} I_{\text{stat}}(\hat{V}_{\text{opt}} \cdot \cos(\omega t)) dt, \quad (1)$$

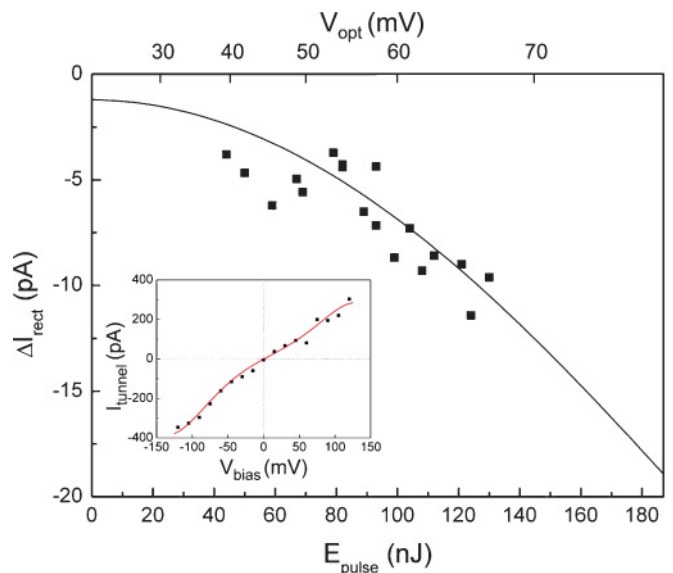


FIG. 3. (Color online) Pulse energy dependence of the change of the tunneling current of “Fast” type of signals for  $V_{\text{bias}} = 0$  V. The dots and the solid line represent measured values and the result of the calculation, respectively. The inset shows the measured static  $I$ - $V$  characteristics (dots) and the polynomial fit (solid red line) used in the calculation.

at  $V_{\text{bias}} = 0$  V and at a given laser frequency  $\omega$ . Here,  $\hat{V}_{\text{opt}}$  represents the amplitude of the optical voltage across the tunneling junction generated by the plasmon field. In order to carry out this integration we approximated the static characteristics with a polynomial function as we measured the static characteristics at discrete bias voltages (see inset of Fig. 3).

On the other hand, assuming a simple one-dimensional (1D) geometry,  $\hat{V}_{\text{opt}}$  can be estimated from the plasmon field amplitude as

$$\hat{V}_{\text{opt}} = \int_0^d \hat{E}_{\text{SP}}(z) dz = \int_0^d \eta \cdot \hat{E}_L \cdot \exp(-\alpha z) dz, \quad (2)$$

where  $\hat{E}_{\text{SP}}$  and  $\hat{E}_L$  represent the amplitudes of the plasmon and the laser field, respectively,  $d$  is being the tip-sample distance,  $\eta$  the electric field enhancement factor and  $\alpha$  the inverse decay length. As  $\alpha^{-1}$  is typically at least by two orders of magnitude larger<sup>24</sup> than typical tunneling distances (in the order of a few tens of Ångströms<sup>25</sup>) we can assume that the electric field of the plasmons is constant across the tunneling junction. Therefore, Eq. (2) simplifies to

$$\hat{V}_{\text{opt}} \approx d \cdot \eta \cdot \hat{E}_L. \quad (3)$$

This means that the measured tunneling currents can be directly related to the estimated SP field amplitudes via  $\hat{V}_{\text{opt}}$ ,  $\eta$  being the *only* fit parameter. We obtained the best fit at  $\eta \approx 390$  (solid line in Fig. 3) suggesting that a field enhancement of about two orders of magnitude is required to generate the measured amount of rectified current at the observed static characteristics. This estimation is in reasonable agreement with values reported earlier in the literature<sup>24,26</sup> but seems to be much higher than the calculated values for an ideally flat Au surface<sup>7</sup> (of a factor of 30). This suggests that nanoscale surface structures play an essential role in the localization of SPs.

We also performed the above calculation for the “Slow” type of signals. The results show that the rectified current component  $\Delta I_{\text{rect}}$  remains constant (in the order of a few pA with negative sign) for a wide range of pulse energies (up to about 100 nJ). Experimental results show, however, rather positive values in the order of a few tens of pA. This observation suggests that in this case the rectified current component remains negligible and thermal effects have a dominant influence on the tunneling current.

#### D. Surface analysis

In order to study the location dependence of the “Fast” signals we extended our point-by-point measurements to two-dimensional surface scans. In addition to the topography signal, we recorded simultaneously transient changes of the tunneling current and applied the time gates described in Sec. III B to them [see also Fig. 2(a)]. The results are depicted in Fig. 4 that shows a “modified topography” image of the  $200 \times 200$  nm<sup>2</sup> surface scan. Here, we highlighted those locations on the conventional topography image where the SP-induced change of the tunneling current ( $\Delta I_{\text{tunnel}}$ ) was observed to be *negative* at  $V_{\text{bias}} = +5$  mV bias voltage, independently on the scanning direction. In other words, the highlighted areas represent the occurrence of “Fast” signals.

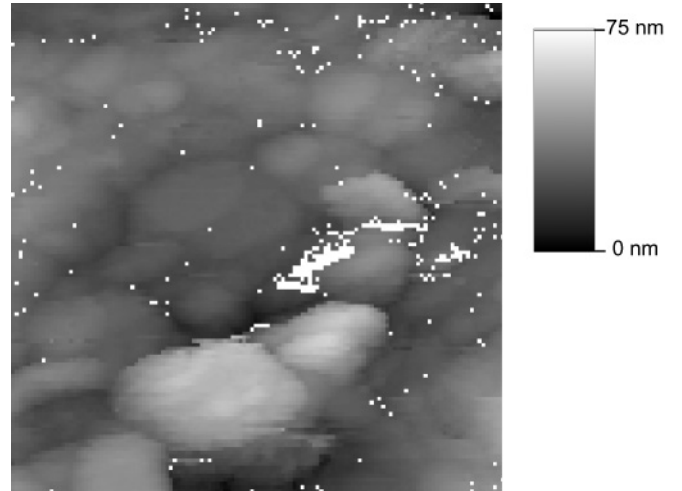


FIG. 4. Modified topography image. Scan size is  $0.2 \times 0.2$   $\mu\text{m}^2$ , resolution  $128 \times 128$  pixels,  $V_{\text{bias}} = +5$  mV,  $I_{\text{set}} = 16$  pA. The highlighted areas represent those locations where the SP-induced change of the tunneling current became negative (i.e., indication of “Fast”-type signals). Each pixel represents an averaged signal resulting from 24 laser pulses.

The observed emergence of negative signals in nanogaps (in our measurement *only* in gaps!) supports the existence of so-called gap plasmon modes.<sup>27</sup> These plasmonic “hot spots” typically appear at grain boundaries or between closely spaced surface nanostructures and are characterized by extremely confined near fields. Theoretical investigations predict field enhancement factors of up to four orders of magnitude in narrow gaps (of a few nm in width).<sup>22</sup> Our results show that the adequate local enhancement of the laser-induced plasmon field along with the nonlinearities in the STM junction give rise to the generation of rectified currents that are sufficient to overcome the DC bias component.

#### IV. SUMMARY

In summary, we demonstrated a set of experiments when surface plasmon (SP) waves were present in the tunneling junction of an STM microscope. The results show that surface topography predominantly determines the magnitude of the local field enhancement. Depending on the surface location, different types of signals can be detected. The signal form (“Slow” or “Fast”) gives indication to the origin of the signal (thermal or plasmon, respectively). The measured signals were externally controlled by varying (a) the electric field of the STM tip (via bias voltage) or (b) the electric field of the optical irradiation (via laser pulse energy). The polarity independence of the “Fast” type of signals in a wide range of bias voltages suggests that they originate from the rectification of the SP field. The analysis of the laser pulse energy dependence allowed us to estimate the local field enhancement that is in the range of two orders of magnitude. Local probing of the confined SP fields shows a pronounced correlation with the surface topography, where the highest enhancement factors were found in gaps as narrow as a few tens of nanometers.

We proved the capability of the STM for characterizing the local SP field enhancement. This could be advantageous

in the optimization of the surface geometry design of high-energy monoenergetic electron sources where ponderomotive acceleration of electrons takes place in the SP field. Further experimental studies with improved spatial resolution (e.g., by using a metal-coated carbon nanotube or Si tip which are better suited for locally probing high-aspect-ratio gaps) may give further insight into the SP localization process.

### ACKNOWLEDGMENTS

We acknowledge the inspiring scientific discussions with Wolfgang Krieger, Fritz Keilmann, Rudolf Gáti, and Prof. Ferenc Krausz and the experimental support of Anton Horn. M.L. was supported by Marie Curie European Reintegration Grant No. MERG-CT-2007-204172 and the OTKA Grants No. PD-72960 and No. 81364.

\*Corresponding author: lenner@szfki.hu

<sup>1</sup>R. Wiesendanger, *Scanning Probe Microscopy and Spectroscopy* (Cambridge University Press, Cambridge, 1994).

<sup>2</sup>D. M. Eigler and E. K. Schweitzer, *Nature (London)* **344**, 524 (1990).

<sup>3</sup>T. Gutjahr-Loser, A. Hornsteiner, W. Krieger, and H. Walther, *J. Appl. Phys.* **85**, 6331 (1999).

<sup>4</sup>W. Krieger, T. Suzuki, M. Völcker, and H. Walther, *Phys. Rev. B* **41**, 10229 (1990).

<sup>5</sup>X. W. Tu, J. H. Lee, and W. Ho, *J. Chem. Phys.* **124**, 021105 (2006).

<sup>6</sup>R. Möller, U. Albrecht, J. Boneberg, B. Koslowski, P. Leiderer, and K. Dransfeld, *J. Vac. Sci. Technol. B* **9**, 50 (1990).

<sup>7</sup>H. Raether, *Surface Plasmons on Smooth and Rough Surfaces and on Gratings* (Springer Verlag, Berlin, 1988).

<sup>8</sup>M. Specht, J. D. Pedarnig, W. M. Heckl, and T. W. Hänsch, *Phys. Rev. Lett.* **68**, 476 (1992).

<sup>9</sup>U. D. Keil, T. Ha, J. R. Jensen, and J. M. Hvam, *Appl. Phys. Lett.* **72**, 3074 (1998).

<sup>10</sup>J. Kupersztych, P. Monchicourt, and M. Raynaud, *Phys. Rev. Lett.* **86**, 5180 (2001).

<sup>11</sup>P. Dombi and P. Rácz, *Opt. Express* **16**, 2887 (2008).

<sup>12</sup>D. R. Ward, F. Hüser, F. Pauly, J. C. Cuevas, and D. Natelson, *Nature Nanotech.* **5**, 732 (2010).

<sup>13</sup>N. Kroó, J. P. Thost, M. Völcker, W. Krieger, and H. Walther, *Europhys. Lett.* **15**, 289 (1991).

<sup>14</sup>R. Huber, M. Koch, and J. Feldmann, *Appl. Phys. Lett.* **73**, 2521 (1998).

<sup>15</sup>L. Arnold, W. Krieger, and H. Walther, *Appl. Phys. Lett.* **51**, 786 (1987).

<sup>16</sup>V. Gerstner, A. Thon, and W. Pfeiffer, *J. Appl. Phys.* **87**, 2574 (2000).

<sup>17</sup>N. M. Amer, A. Skumanich, and D. Ripple, *Appl. Phys. Lett.* **49**, 137 (1986).

<sup>18</sup>N. W. Mermin and N. D. Ashcroft, *Solid State Physics* (Thomson Brooks/Cole, Pacific Grove, 1976).

<sup>19</sup>A. V. Bragas, S. M. Landi, and O. E. Martinez, *Appl. Phys. Lett.* **72**, 2075 (1998).

<sup>20</sup>S. I. Bozhevolnyi, V. S. Volkov, and K. Leosson, *Phys. Rev. Lett.* **89**, 186801 (2002).

<sup>21</sup>J. Kim, G. L. Liu, Y. Lu, and L. P. Lee, *Opt. Express* **13**, 8332 (2005).

<sup>22</sup>H. Xu, J. Aizpurua, M. Käll, and P. Apell, *Phys. Rev. E* **62**, 4318 (2000).

<sup>23</sup>Y. Kuk, R. S. Becker, P. J. Silverman, and G. P. Kochanski, *Phys. Rev. Lett.* **65**, 456 (1990).

<sup>24</sup>S. E. Irvine, P. Dombi, Gy. Farkas, and A. Y. Elezzabi, *Phys. Rev. Lett.* **97**, 146801 (2006).

<sup>25</sup>H. Q. Nguyen, P. H. Cutler, T. E. Feuchtwang, Z. H. Huang, Y. Kuk, P. J. Silverman, A. A. Lucas, and T. E. Sullivan, *IEEE Trans. Electron Devices* **36**, 2671 (1989).

<sup>26</sup>M. Moskovits, *Rev. Mod. Phys.* **57**, 783 (1985).

<sup>27</sup>R. Hillenbrand and F. Keilmann, *Appl. Phys. B* **73**, 239 (2001).